$$J_{sc} = \left[-kT \int_0^L \frac{1}{\sigma} \left(\frac{d\sigma_p}{dx} - \frac{d\sigma_n}{dx} \right) dx + \int_0^L \frac{\Delta\sigma}{\sigma} E_0 \, dx - \int_0^L \frac{\Delta\sigma_n}{\sigma} \frac{d\chi}{dx} dx - \int_0^L \frac{\Delta\sigma_p}{\sigma} \frac{d(\chi + E_G)}{dx} \right] \left(\int_0^L \frac{dx}{\sigma} \right)^{-1}. \quad (10)$$

Equation (10) shows that contributions of the various effects have roughly the same relative importance as in the case of the contributions to V_{oc} given by Eq. (9). It should be noted that $\Delta p(x)$ and $\Delta n(x)$ under open- and short-circuit conditions could be very different and so

$$\frac{J_{sc}}{V_{oc}} \neq \left(\int_0^L \frac{dx}{\sigma} \right)^{-1}.$$

Solar cells produced on a-Si : H almost invariably use the MS or MIS Schottky barrier structure because of difficulty in making p-n junctions. In these devices the primary attribute of photoconduction has been recognized by several workers as the reduction in series resistance under light.[8] Certain Schottky barrier solar cells on a-Si : H have exhibited unusually high values of V_{oc} (as high as 0.8 eV) and this has been ascribed to thin oxide formation at the interface resulting in an MIS structure.[9,10] This paper has pointed out certain additional contributions to V_{oc} and J_{sc} that can arise from photoconductivity in regions outside the barrier, due to impurity or compositional grading. Exploitation of these effects in novel structures could provide a singular boost to solar-cell efficiency.

In summary, Eq. (9) lists the origins of photovoltaic action. It explicitly shows the interrelation between photoconduction and photovoltaics. In conventional photovoltaic materials, photoconduction is only appreciable in depleted barrier regions. Hence Eq. (9) shows that for these materials under light the principal contribution to V_{oc} comes from such barrier regions, i.e., basically from the electric field existing in these regions in thermodynamic equilibrium. Other contributions to V_{oc} can be present (e.g., from built-in electric fields) but these will tend to be of secondary importance in conventional nonphotoconductive materials since $e\mu_n \Delta n/\sigma$, etc., are very small in regions outside depleted areas. In photoconductive materials $e\mu_n \Delta n/\sigma$, $e\mu_p \Delta p/\sigma$, etc. can be large throughout the material. Built-in fields, electron affinity variations, and hole affinity variations can now make primary contributions to V_{oc} wherever they exist.

The Denber contribution in Eq. (9) must always be examined in these cases, however, since it can add or subtract from these effects.

[1] J.I. Pankove, *Optical Processes in Semiconductors* (Dover, New York, 1971).
[2] P.J. Zanzucchi, C.R. Wronski, and D.E. Carlson, J. Appl. Phys., **48**, 5227 (1977).
[3] J.E. Sutherland and J.R. Hauser, IEEE Trans. Electron Devices **ED-24**, 363 (1977).
[4] Y. Marfaing and J. Chevallier, IEEE Trans. Electron Devices **ED-18**, 465 (1971).
[5] S.J. Fonash, CRC Crit. Rev. Solid-State Mater. Sci. (to be published).
[6] I. Solomon and J. Perrin, Proc. 14th Internat. Conf. Physics of Semiconductors Edinburgh, England, 1978 (unpublished).
[7] S. Ovshinsky, New Scientist, **80**, 674 (1978).
[8] C.R. Wronski, *IEEE* Trans. Electron Devices **ED-24**, 351 (1977).
[9] D.E. Carlson, ibid, 449 (1977).
[10] D.E. Carlson (private communication).

Direct injection readout of the *p*-*n* PbS-Si heterojunction detector

A. J. Steckl, K. Y. Tam, and M. E. Motamedi
Electrical and Systems Engineering Department, Rensselaer Polytechnic Institute, Troy, New York 12181

(Received 21 May 1979; accepted for publication 16 July 1979)

An n-channel MOSFET circuit implemented within a CMOS structure has been used to test the feasibility of integrating the infrared signal readout within a PbS-Si heterojunction detector (HJD) array. The efficiency of the source-coupled direct injection readout was determined from $\eta_{\rm inj} = I'_{\rm ph}/I_{\rm ph}$, where $I'_{\rm ph}$ is the photocurrent measured with the direct injection readout and $I_{\rm ph}$ is the photocurrent measured with a virtual ground transimpedance amplifier. From the equivalent circuit of the direct injection input, the theoretical injection efficiency at low frequency has been shown to be $\eta_{\rm inj} = g_m(g_m + G_D)^{-1}$, where g_m is the MOSFET transconductance and G_D is the detector conductance. Good agreement between the experimental and theoretical injection efficiency has been found over a wide range. Injection efficiencies as high as 90% have been measured.

PACS numbers: 72.40. + w, 73.40.Lq, 73.60.Fw

The PbS-Si heterojunction detector (HJD) has been shown[1,2] to exhibit substantial IR detectivity reaching $(1\text{–}2)\times 10^{11}$ cm Hz$^{1/2}$/W in the 2.5–3.0 μm region. Techniques for the integration of the PbS-Si HJD in a focal plane array which contains its own readout circuit in the form of a MOSFET X-Y address array or a CCD array have been re-

Downloaded 07 Oct 2003 to 129.137.210.120. Redistribution subject to AIP license or copyright, see http://ojps.aip.org/aplo/aplcr.jsp

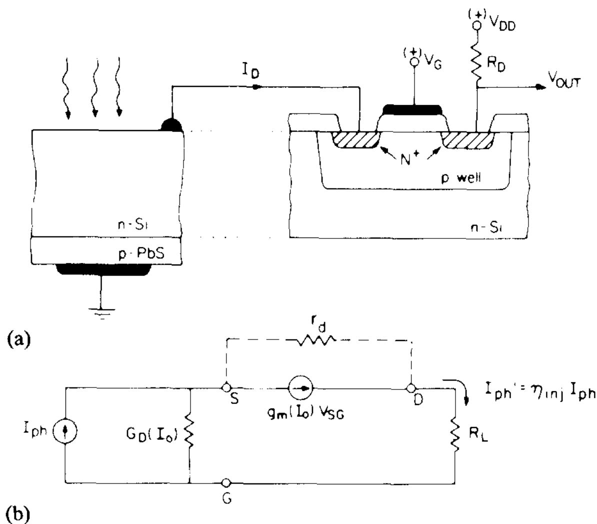

FIG. 1. PbS-Si HJD readout configuration. (a) Structure cross-section and interconnection, (b) small-signal equivalent circuit model.

cently discussed.[3] Basically, both integration techniques involve the fabrication of an MOS circuit on the backside of the same Si substrate on which the PbS-Si HJD is formed. In the case of the anisotype (*p-n*) PbS-Si HJD, the IR-generated photocarrier of interest is the photoelectron generated in the PbS near the PbS-Si interface.[3,4] Under reverse bias, this photoelectron is injected into the Si substrate. In order to readout these carriers, *n*-channel devices have to be fabricated on the *n*-Si substrate.

A Si chip with a CMOS structure containing both *n*- and *p*-channel devices, with the former being formed inside a *p* well, has been designed and fabricated[5] to investigate the feasibility of the basic integration technique. The PbS-Si HJD is connected to the readout MOSFET in the source-coupled direct injection mode, as shown in Fig. 1(a). The readout operation was characterized as a function of photosignal intensity, detector bias current, and temperature.

The injection efficiency of the readout was determined

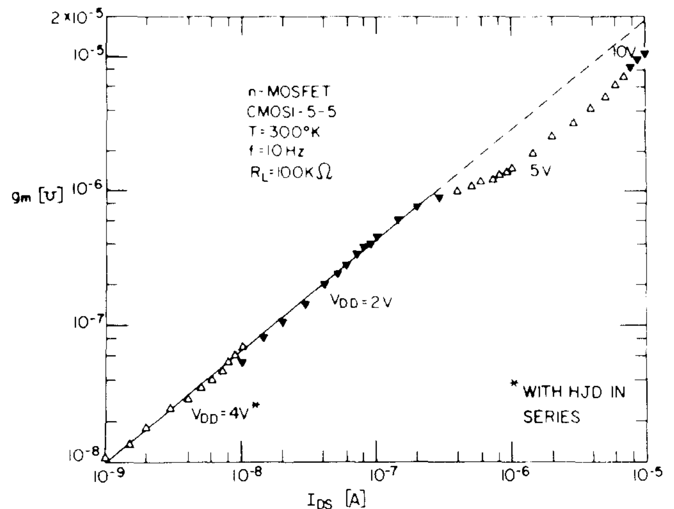

FIG. 3. MOSFET transconductance as a function of drain-source current.

from the $\eta_{inj} = I'_{ph}/I_{ph}$ ratio, where I'_{ph} is the photocurrent measured with the direct injection readout and I_{ph} is the photocurrent measured with a virtual ground transimpedance preamplifier. From the small-signal equivalent circuit of the direct injection readout [Fig. 1(b)] the theorectical injection efficiency can be shown[6,7] to be $\eta_{inj} = g_m(g_m + G_D)^{-1}$ at low frequency, where g_m is the input transconductance of the readout MOSFET and G_D is the detector conductance.

The small signal detector conductance measured as a function of dc reverse bias current is shown in Fig. 2. At 300 °K, G_D is seen to vary almost linearly with I_0, showing the absence of current saturation. At 93 °K, G_D is relatively constant, varying only around a factor of 2 over the 10^{-9}–10^{-7} bias current range.

The readout MOSFET was designed with $W/L = 6$. However, due to the low detector bias current, the MOSFET was generally operated in the subthreshold regime. In this region, the transconductance is directly proportional[7,8] to drain (bias) current, $g_m \sim qI_0/kT$. The transconductance of the *n* MOSFET used in the readout experiments is shown in

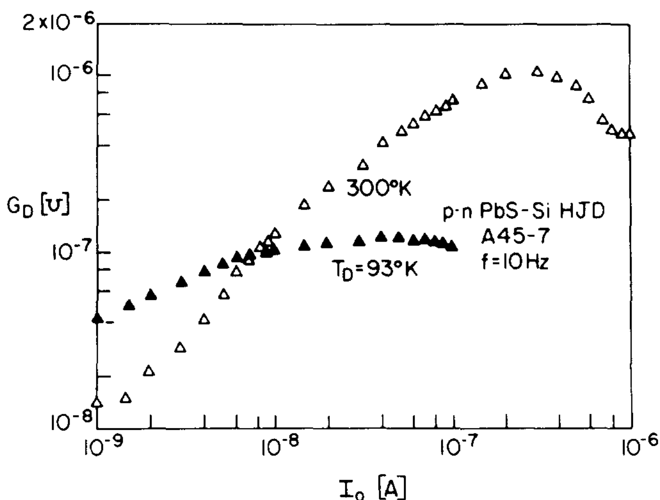

FIG. 2. PbS-Si HJD conductance as a function of dc bias current.

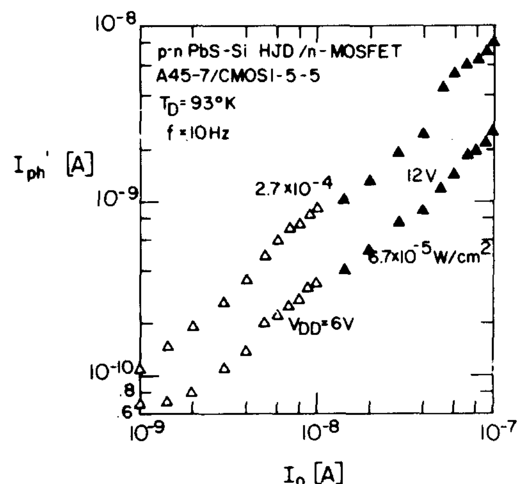

FIG. 4. Injected photocurrent as a function of dc bias current.

Downloaded 07 Oct 2003 to 129.137.210.120. Redistribution subject to AIP license or copyright, see http://ojps.aip.org/aplo/aplcr.jsp

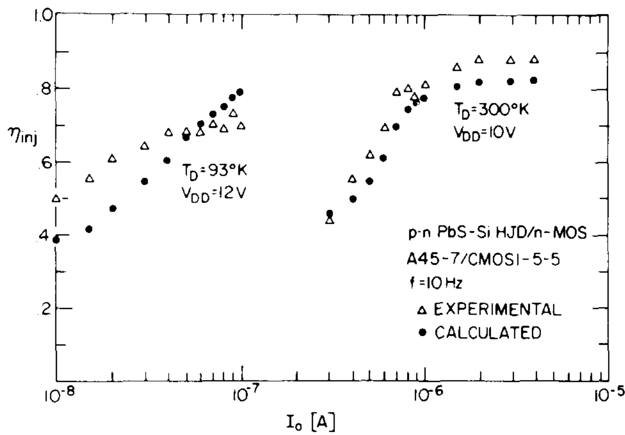

FIG. 5. Injection efficiency as a function of dc bias current at 93 and 300 °K.

Fig. 3 as a function of drain current. I_{DS} was varied four orders of magnitude by adjusting the drain voltage as indicated in Fig. 3. For drain current levels between 10^{-9} and 10^{-7} A, g_m is indeed seen to be approximately proportional to I_{DS}. Above 10^{-7} A, a deviation from the simple linear relation is observed.

The n-MOSFET readout of the IR signal generated by the PbS-Si HJD was characterized as a function of the dc bias current at various levels of incident power. In Fig. 4, the injected photocurrent obtained at $T_D = 93$ °K and $f = 10$Hz is plotted versus I_0 at $H_{BB} = 6.7\times10^{-5}$ and 2.7×10^{-4} W/cm^2. The black-body temperature was 1000 °C and a filter was used to prevent photocurrent generation in the Si substrate. As before, in order to vary I_0 over a wide range, more than one value of V_{DD} was used. By comparing I'_{ph} with the photocurrent measured with a transimpedance amplifier (PAR 181), the injection efficiency is obtained. In Fig. 5, η_{inj} is plotted versus I_0 for both low-temperature (93 °K) and room-temperature operation. Comparing the experimental values of the injection efficiency (I'_{ph}/I_{ph}) to those obtained from the model $[g_m/(g_m + G_D)]$, it can be noted that good agreement is obtained at 300 °K, while a fair agreement is seen at 93 °K. In general, η_{inj} increases with the bias current. This behavior is the combined effect of I_0 on g_m and G_D, as seen in Figs. 2 and 3.

In conclusion, the feasibility of integrating PbS-Si heterojunction detectors with Si MOS readout structures has been demonstrated. The injection efficiency of the source-coupled direct injection mode has been investigated and values as high as 90% have been obtained.

[1]A.J. Steckl, H. Elabd, and T. Jakobus, Tech. Digest IEDM 1977 IEEE Cat. No. 77CH 12757 ED, pp. 549–550 (unpublished).
[2]S.P. Sheu and A.J. Steckl, Proc. Intl. Conf. on Infrared Physics, Zurich, 1979, pp. 351–353 (unpublished).
[3]A.J. Steckl, M.E. Motamedi, S.P. Sheu, H. Elabd, and K.Y. Tam, Proc. CCD 1978 Conf., San Diego, pp. 239–250 (unpublished).
[4]A.J. Steckl and S.P. Sheu (unpublished).
[5]M.E. Motamedi. K.Y. Tam, and A.J. Steckl, Proc. Custom Integrated Circuits Conf., Rochester, 1979 (unpublished).
[6]A.J. Steckl, Proc. CCD 1975 Conf., San Diego pp. 85–93 (unpublished).
[7]J. Longo, D.T. Cheung, A.M. Andrews, C.C. Wang, and J.M. Tracy, Trans. Electron. Devices **ED-25**, 213–232 (1978).
[8]E.D. Johnson, RCA Rev. **34**, 80–94 (1973).

Highly doped evaporated amorphous silicon by alkali implantation

W. Beyer,[a] A. Barna,[b] and H. Wagner
Fachbereich Physik der Universität Marburg, Renthof 5, D-3550 Marburg, Germany

(Received 13 April 1979; accepted for publication 19 July 1979)

Evaporated films of amorphous silicon can be doped interstitially by implantation of alkali ions. Room temperature conductivity values as high as $\sigma = 2\times10^{-3}\,(\Omega\,\mathrm{cm})^{-1}$ and activation energies of σ as low as 0.25 eV are obtained by implantation of 1% potassium in films prepared with a low rate of deposition. The doped state is stable up to 320°C. Results from stepwise doping with sodium indicate a rather constant density of localized states in the gap of the order 3×10^{19}/cm^3 eV for rapidly evaporated films.

PACS numbers: 72.80.Ng, 72.20.Pa, 61.70.Tm, 66.30.Jt

Amorphous silicon (a-Si) prepared by evaporation has long been considered rather insensitive to doping, in contrast to material deposited by glow-discharge decomposition of silane.[1] Recently we have shown, however, that also evaporated a-Si films can be doped by implantation and in-diffusion of interstitial lithium.[2] Yet, the Li-doped state was found to be rather unstable. Above 200 °C the doping effect disappears rapidly by out-diffusion and precipitation effects connected to the high diffusivity of lithium.[3] Aiming to investigate if evaporated films of a-Si can be doped thermally stable to conductivity values as high as glow-discharge material, it was tempting to try implantation of heavier alkali ions (e.g. Na$^+$, K$^+$) instead, which are known to act as donors in crystalline Si as well[4] but have a lower diffusion constant.

[a]Present address: Institut für Grenzflächenforschung und Vakuumphysik der Kernforschungsanlage Jülich GmbH, D-5170 Jülich, Germany.
[b]Permanent address: Research Institute for Technical Physics of the Hungarian Academy of Sciences, Budapest, Hungary.

Downloaded 07 Oct 2003 to 129.137.210.120. Redistribution subject to AIP license or copyright, see http://ojps.aip.org/aplo/aplcr.jsp